Separation Mechanisms for Nanoscale Spheres and Rods in Field-Flow Fractionation

Frederick R. Phelan Jr.* and Barry J. Bauer**

*Polymers Division, NIST, Gaithersburg, MD, USA, frederick.phelan@nist.gov
**Polymers Division, NIST, Gaithersburg, MD, USA, barry.bauer@nist.gov

ABSTRACT

Separation mechanisms for spheres and rodlike particles in classical field-flow fractionation (FFF) are studied using a Brownian dynamics simulation. For spheres, simulation results for mean elution time are found to be in good agreement with experimental data and the steric inversion theory of Giddings [1]. Modeling of particle separation for rods is compared with spheres of equal diffusivity. The simulation shows that nanotube scale particles elute by a normal mode mechanism up to aspect ratios of about 500, based on a particle diameter of 1 nm. At larger sizes, the rods also show a steric deviation from normal mode elution, but in the opposite sense as for spheres. The different behavior is attributable to the effect of particle shape. Extension of the steric mode theory for spheres to rods illustrates a potential steric mode separation that can be used to separate rods based on chirality.

Keywords: Brownian Dynamics, Field-Flow Fractionation, Nanotubes, Separations, SWNT

1 INTRODUCTION

For nanotubes to achieve their full potential in applications, it is desirable to be able to separate them according to their various physical properties. One possible technique for achieving this is field-flow fractionation (FFF), depicted in Figure 1.

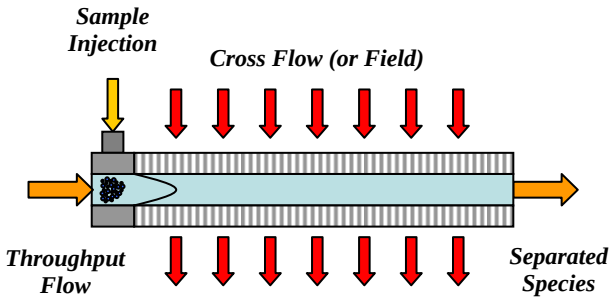

Figure 1: Schematic of frit-inlet symmetrical, field-flow fractionation. In the asymmetric variation, only the lower wall is porous.

Classical flow-FFF is a separation technique in which a perpendicular cross flow is imposed upon a channel flow of dilute particulates [1-3]. The cross flow exits through a porous accumulation wall which is impermeable to the particulates. Competition between various flow mechanisms drives particles of unlike size to different average positions in the cross flow direction. Separation is achieved due to the different residence times of the particles based upon their position in the parabolic velocity profile in the throughput direction. FFF can also be combined with other techniques such as dielectrophoresis to produce separations based on electronic, as well as size based properties.

A number of different mechanisms can be exploited to achieve separation in flow-FFF. Normal mode separation applies to particles which are small enough to undergo significant Brownian motion, and whose size is small compared to the cross flow gap size. In this case, smaller particles, which are more diffusive, have an average position closer to the centerline and elute faster than larger particles. Steric mode separation occurs when the particle layer in FFF is strongly compressed along the accumulation wall. In this case for spheres, larger particles are more highly entrained by the throughput flow and elute more quickly than smaller ones. This turnaround is called steric inversion.

Particle separation in flow-FFF can be described by a theoretical variable called the retention, R, which represents the ratio of the average residence time of non-retained tracers, t_0, to the average retention time of the particles, t_r, *i.e.*, $t_r = t_0 / R$, where $0 \le R \le 1$. For the case of normal mode separation, the retention is given by

$$R = 6\lambda\left[\coth\left(\frac{1}{2\lambda}\right) - 2\lambda\right] \qquad (1.1)$$

where λ is an inverse Peclet Number (Pe) given by

$$\lambda = \frac{D}{|v_c| H} = \frac{1}{Pe} \qquad (1.2)$$

v_c is the cross flow velocity, D is the diffusion coefficient of the particle in the cross flow direction, and H is the cross-flow thickness. A model which takes into account both normal mode diffusion and steric effects for spheres in FFF derived by Giddings [1]

$$R = 6\left(\alpha - \alpha^2\right) + 6\lambda\left(1 - 2\alpha\right)\left[\coth\left(\frac{1-2\alpha}{2\lambda}\right) - \frac{2\lambda}{1-2\alpha}\right] \qquad (1.3)$$

where α is the ratio of the particle radius to gap thickness, *i.e.*, $\alpha = r / H$. For the case of negligible particle size, Eq.

(1.3) reduces to Eq. (1.1). It can be seen that, theoretically, normal mode elution is independent of the particle shape and depends only on the particle diffusion coefficient. Steric mode separations become independent of diffusion, but little is known about how steric mode separations are effected by different particle shapes.

In what follows, a Brownian dynamics simulation is used to investigate the separation of spheres and rodlike particles in flow-FFF. First, we study the case of spheres to validate the simulation method by comparison with experimental data and existing theory. We then compare simulation results for rods with spheres of equal diffusivity and show that the difference in particle shape leads to divergent trends at large particle size in the steric mode regime. Finally, we look at the elution of oriented rods and elucidate a potential steric mode separation that can be used to separate rods based on chirality.

2 SIMULATION

In this work, we have developed a Brownian dynamics simulation to investigate the separation of spheres and rodlike particles in flow-FFF. A summary of pertinent details of the numerical method are discussed below. Full details are found in references [4-6].

2.1 Model Equations

For spheres, the particle motions are governed by a Langevin equation which takes into account the drag force due to fluid flow and the Brownian force [7,8]. The linear momentum balance for an ensemble of spheres in a viscous flow, individually denoted by the superscript (i), is given by the Langevin equation

$$\frac{d}{dt}\left(\underline{R}^{(i)}\right) = \underline{v}\left(\underline{R}^{(i)}\right) + \frac{\underline{F}_B^{(i)}(t)}{\zeta^{(i)}} \tag{1.4}$$

where $\underline{R}$ is the position vector of the particle, $\underline{v}\left(\underline{R}\right)$ is the unperturbed velocity of the fluid evaluated at the particle position, $\underline{F}_B$ is the random force due to Brownian motion, and ζ is the Stokes' law drag coefficient given by

$$\zeta = 6\pi r\eta \tag{1.5}$$

where r is the particle radius, and η is the fluid viscosity.

Rods are modeled as prolate ellipsoids. The particle motions are governed by a similar Langevin equation with orientation dependent drag and diffusion coefficients, and the Jeffrey equation with rotational diffusion [4,7,8]

$$\frac{d}{dt}\left(\underline{R}^{(i)}\right) = \underline{v}\left(\underline{R}^{(i)}\right) + \left[\underline{\underline{\zeta}}^{(i)}\right]^{-1} \cdot \underline{F}_B^{(i)} \tag{1.6}$$

$$\frac{d}{dt}\left(\underline{p}^{(i)}\right) = -\underline{\underline{W}} \cdot \underline{p}^{(i)} + \lambda_p^{(i)}\left(\underline{\underline{D}} \cdot \underline{p}^{(i)} - \underline{\underline{D}} : \underline{p}^{(i)}\underline{p}^{(i)}\underline{p}^{(i)}\right) + \underline{p}^{(i)} \times \left[\underline{\underline{\xi}}^{(i)}\right]^{-1} \cdot \underline{\mathrm{T}}_B^{(i)} \tag{1.7}$$

where $\underline{R}$ and $\underline{p}$ are the position and orientation vectors of the particles, $\underline{F}_B$ and $\underline{\mathrm{T}}_B$ are the Brownian force and torque, $\underline{\underline{\zeta}}$ and $\underline{\underline{\xi}}$ are hydrodynamic resistance tensors, $\underline{\underline{D}}$ and $\underline{\underline{W}}$ are the stretching and vorticity tensors, respectively, $\lambda_p = \frac{\Re^2 - 1}{\Re^2 + 1}$ and $\Re = \frac{a}{b}$.

2.2 Boundary Conditions

An important part of the scheme is the interaction of the particles with the boundaries. The cross flow velocity continually drives the particles towards the accumulation wall and the diffusion step being random may also cause the particles to collide with or overstep this boundary. To handle this, a no-penetration boundary condition is used. For spheres, particles may only approach within a distance equal to one particle radius of the upper and lower boundaries. For rods, a similar criterion based on the rod size and 3-D orientation is used [6].

3 RESULTS

3.1 Spheres

Modeling and experimentation of particle separation for spheres under conditions spanning the normal to steric transition was examined. The goal of this was to test the simulation model by comparison with experimental data and existing theory. The experimental procedure is described in reference [5]. Results are shown in Figure 2 and Table 1. Both the simulation results and experimental data for mean elution time are in good agreement with the steric inversion theory of Giddings, *i.e.*, Eq. (1.3). For the given experimental conditions, the steric transition occurs when the particle diameter is in the range 300 to 600 nm, with full steric inversion at 600 nm.

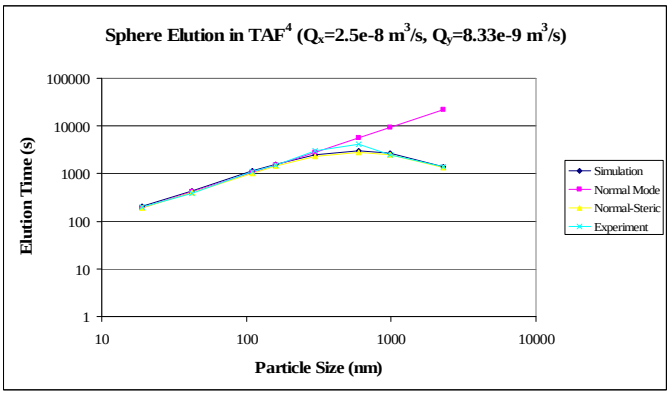

Figure 2: Comparison of simulation elution times with experimental data and theory [5].

NSTI-Nanotech 2008, www.nsti.org, ISBN 978-1-4200-8503-7 Vol. 1

3.2 Brownian Rodlike Particles

In this section we consider the modeling of rodlike particles which are subject to both translational and rotational diffusion, shown schematically in Figure 3.

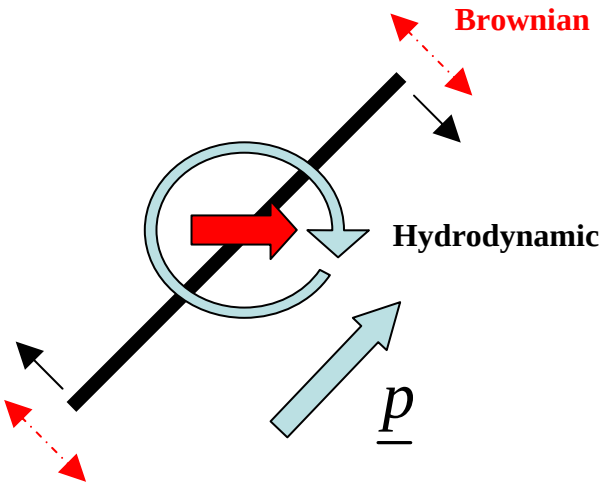

Figure 3: Forces on a rodlike particle subject to both shear flow and translational and rotational Brownian motion.

Particle separation for rods is compared with spheres of equal diffusivity as under normal mode conditions such particles should elute at the same rate. The rods are assumed to be 1 nm in diameter. The equivalent diffusion sphere size is given by the expression [6]

$$r_{eq} = a\frac{16}{3}\frac{s^3}{2s+\left(3s^2-1\right)Z} \qquad (1.8)$$

where a and b are the major and minor axes of the ellipse, respectively, $s=\sqrt{a^2-b^2}/a$, and $Z=\ln\left[\left(1+s\right)/\left(1-s\right)\right]$.

Results are shown in Figure 4, which plots the deviation from normal mode theory for the two different particle types as a function of equivalent sphere size. The data show that rods and spheres of equal diffusivity elute at the same rate up to an equivalent sphere size of 90 nm, which corresponds to a rod size of about 500 nm. At larger sizes, the rods begin to deviate from normal mode theory, but in the opposite sense as for spheres. While the steric effect for spheres causes larger spheres to elute faster than predicted by normal mode theory, an inverse steric effect occurs for rods in which larger rods move increasing slower than that predicted by the theory. This occurs due to alignment of the larger, less Brownian rods in low velocity region along the accumulation wall. It can be seen that past sphere:rod sizes of approximately 90 nm:500 nm, the negative steric deviations for the spheres and the positive steric deviations for rods lead to increasingly greater differences in mean elution times for the two different particle types. This can be viewed as a positive result as it shows that nanotubes can be increasingly fractionated by size in flow-FFF.

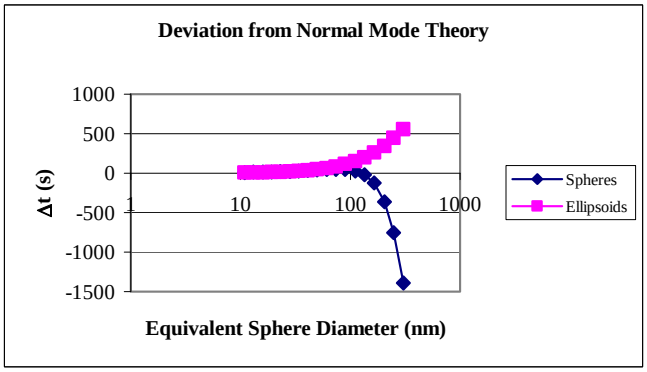

Figure 4: Comparison of the deviation of elution time from normal mode theory for spheres and rods of equal diffusivity.

3.3 Oriented Rodlike Particles

The steric inversion of spheres suggests that an even stronger steric effect might be obtained for rodlike particles due to their great length, if they could be oriented normal to the flow direction. This could be useful in the context of nanotube separation if either metallic or semi-conducting types could be preferentially oriented relative to the other, and could be accomplished by use of an AC electric field to induce alignment, as shown in Figure 5. The torque due to the electric field would have to be strong enough to resist the torque due to shear and the Brownian force.

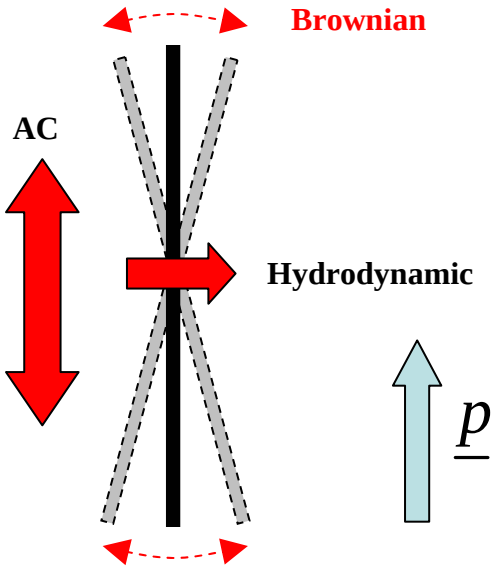

Figure 5: Forces on a rodlike particle subject to both shear flow, translational and rotational Brownian motion, and an AC electric field to induce “wobbly” alignment.

We investigate this in a straightforward manner by modifying Eq. (1.3) with $\alpha' = a/H$, where a is once again the length of the ellipsoid major axis. Results are shown in Figure 6.

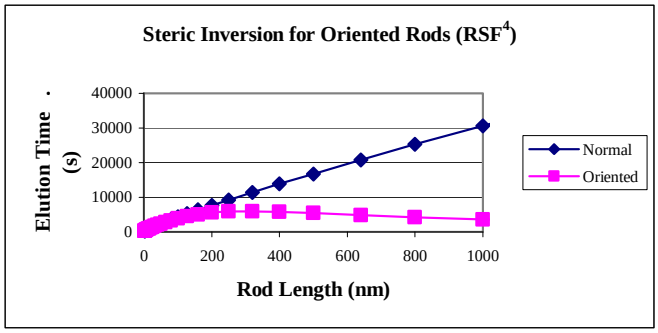

Figure 6: Comparison of elution time for rodlike particles under normal mode conditions, and for rods oriented perpendicular to flow direction.

The results show that oriented rods will exhibit steric inversion. Thus, in the case of mixtures of oriented and Brownian rods, the species can be separated into two fractions. The first fraction will contain oriented rods of all sizes, and Brownian rods whose size is such that their elution time is less than the elution time corresponding to the steric inversion point for the oriented rods. The second fraction will contain the longer Brownian rods. For the case shown in Figure 6, the cutoff size in the first fraction is 150 nm; smaller cutoff sizes can be obtained by optimizing parameter conditions. The first fraction may be further refined using size separation only.

4 SUMMARY AND CONCLUSIONS

We have investigated particle separation mechanisms in flow-FFF using Brownian dynamics method, and comparison with experimental results and theory. The following conclusions can be drawn from the present work.

- Under normal mode conditions, spheres and rods of equal diffusivity elute at the same rate and small particles elute faster than large particles.
- For large sphere sizes, steric inversion occurs due to size exclusion of the particles at the boundary. Past the steric inversion point, large particles elute faster than small particles. The Brownian dynamics results show very good agreement with both theory and modeling on this point.
- Large rods show an inverse steric effect relative to spheres, in which larger rods move increasing slower than that predicted by normal mode theory due to alignment of the rods in low velocity region along the accumulation wall. This can be viewed as a positive result as it shows that nanotubes can be increasingly fractionated by size in flow-FFF.
- Rods oriented normal to the flow direction can be expected to exhibit steric inversion. This suggests a potential mechanism to separate nanotubes based on chirality, if nanotubes of different type can be preferentially oriented in an AC electric field.

REFERENCES

1. J. C. Giddings, Separation Science and Technology **13,** 241 (1978).
2. J. Janca, in *Field-Flow Fractionation*, (Marcel Dekker, New York, 1987).
3. in *Field-Flow Fractionation Handbook*, (Wiley-Interscience, 2000).
4. F. R. Phelan Jr. and B. J. Bauer, Chemical Engineering Science **62,** 4620 (2007).
5. F. R. Phelan Jr. and B. J. Bauer, Analytical Chemistry **submitted,** (2008).
6. F. R. Phelan Jr. and B. J. Bauer, AICHE Journal **submitted,** (2008).
7. A. Satoh, in *Introduction to Molecular-Microsimulation of Colloidal Dispersions*, (Elsevier Science B.V., Amsterdam, The Netherlands, 2003).
8. S. Kim and S. J. Karrila, in *Microhydrodynamics: Principles and selected applications*, (Butterworth-Heinemann, Stoneham, 1991).

5 TABLES

Elution Data for Spheres			
d (nm)	Experiment Mean (s)	Simulation Mean (s)	% diff
19	195	208.6	6.5
42	389	439.6	11.6
110	1080	1121.6	4.0
160	1490	1581.1	5.6
300	2990	2532.7	-17.9
600	4200	3067.3	-36.9
984	2510	2639.3	5.0
2300	1380	1404.2	1.6

Table 1: Comparison of simulation and experiment for spheres [5]. The relative uncertainties reported are one standard deviation, based on the goodness of the fit or from multiple runs.